Supporting Information

Iron-modulated Ni_3S_2 derived from a Ni-MOF-based Prussian blue analogue for highly efficient oxygen evolution reaction

Yaoxia Yang[*,§], Fengyao Guo[§], Lan Zhang, Xingwei Guo, Dangxia Wang,

Ruiqing Niu[a], Haidong Yang, Jian Li, Guofu Ma and Ziqiang Lei

Key Laboratory of Eco-functional Polymer Materials of the Ministry of Education,

Key Laboratory of Eco-environmental Polymer Materials of Gansu Province,

College of Chemistry and Chemical Engineering, Northwest Normal University,

Lanzhou 730070, China.

[*]Corresponding author.

E-mail address: yaoxiayang@nwnu.edu.cn; yangyaoxia2007@126.com (Y-X, Yang).

Experimental Section

Calculation

The specific calculation process for mass activity and turnover frequency (TOF) was as follows:

The values of mass activity (A g^{-1}) were calculated from the catalysts loading m (mg cm^{-2}) and the measured current density j (mA cm^{-2}) at 0.33 V.

$$Mass\ activity\ = \frac{j}{m}$$

Turnover frequency (TOF) calculation

TOF of catalyst was calculated using a method widely used in the literature, e.g. Nano Energy 2018, 51, 26-36. First, the active site (N) of the catalytic electrode was calculated by the following formula:

$$N(mol) = \frac{Q}{2F} = \frac{it}{2F} = \frac{iV/u}{2F}$$

Where, Q represents the voltammetry charge obtained by integrating the cyclic voltammetry curve, CV curve is at a certain sweep velocity (50 mV/s) between -0.2 ~ 0.6 V (vs. RHE) in phosphate buffer solution (PB, pH = 7.0), the PB is prepared by mixing up 38 mL of 0.2 M NaH_2PO_4 solution and 62 mL of 0.2 M Na_2HPO_4; where Q is the cyclic voltammetric capacity obtained by integrating CV cures, F is the Faradic constant (96485 C mol^{-1}), i is the current density (A m^{-2}), V is the voltage (V) and u is the scanning rate (V s^{-1}).

Secondly, Faraday's constant (TOF) is calculated by the following formula:

$$TOF(s^{-1}) = \frac{|j|A}{nFN}$$

Where, j represents the current density at a given overpotential, where the

overpotential is 1.50 V (vs RHE); A represents the geometric area of the electrode; n represents the number of electrons consumed by hydroelectricity to decompose into a O_2, n = 4 in OER process; F stands for Faraday constant (96485 C mol^{-1}); N is the number of active sites.

Gas Chromatography Testing

The Faradaic efficiency (FE) was calculated by using following equation

$$FE = \frac{Nex}{Nth}$$

where Nex is the produced moles of oxygen and Nth is the theoretical moles of oxygen.

Gas chronopotentiometry (GC-9560) testing was conducted with a constant current density of 100 mA cm^{-2} in 1 M KOH seawater electrolyte. The theoretical amount of generated O_2 gases was calculated using the equation:

$$Nth = \frac{It}{4F}$$

Where Nth is the theoretical amount (mol) of gaseous products, I is the current (A), t is the time (s) and F is the Faraday constant.

Fig. S1. Optical photographs of the Ni-MOF/NF, Ni-MOF@PBA/NF and the Fe-Ni_3S_2/NF with the size of 1.0 × 2 cm^2.

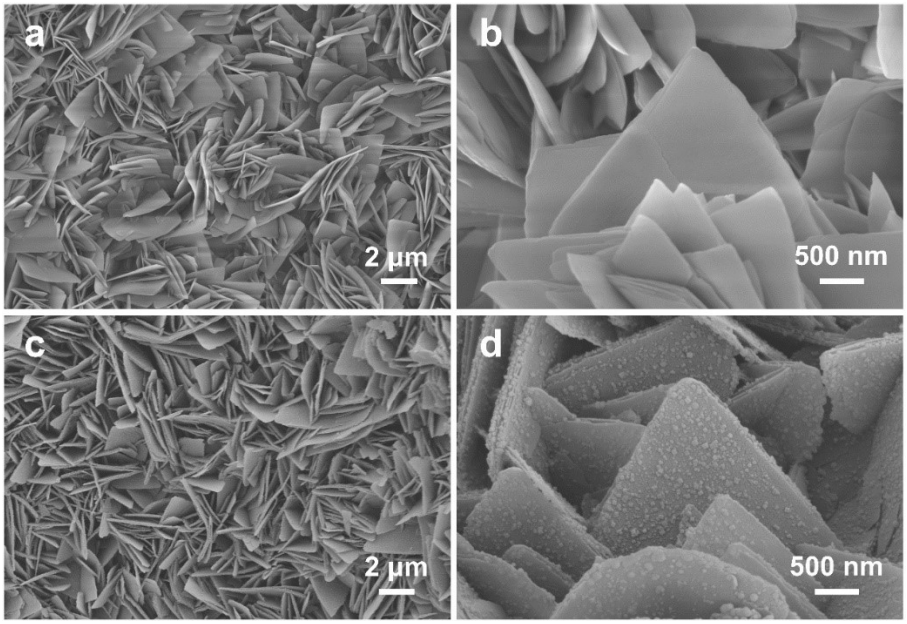

Fig. S2. SEM images of (a, b) Ni-MOF/NF, (c, d) Ni-MOF@PBA/NF.

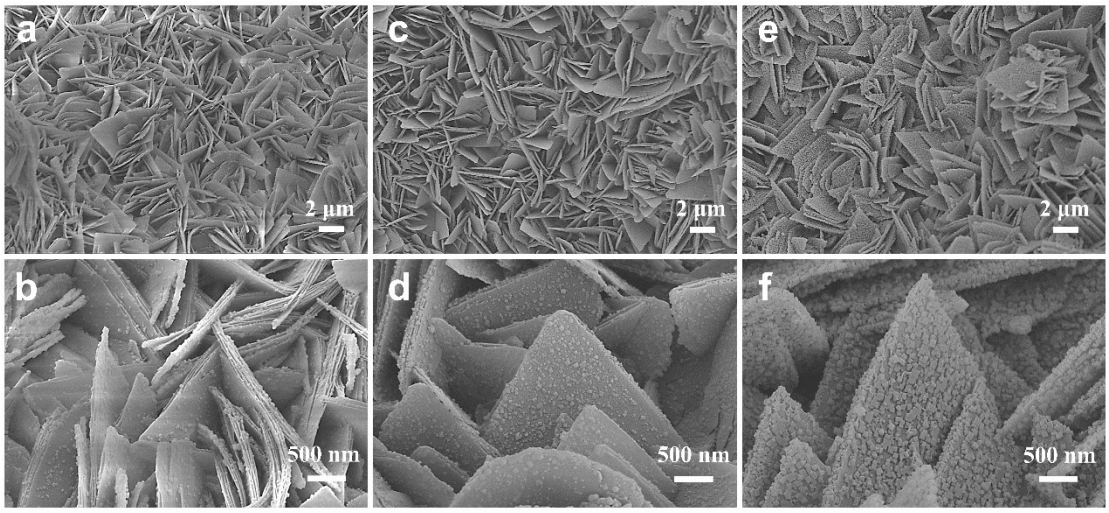

Fig. S3. SEM images of Ni-MOF@PBA/NF synthesized at room temperature for (a, b) 3 h, (c, d) 6 h, (e, f) 12 h.

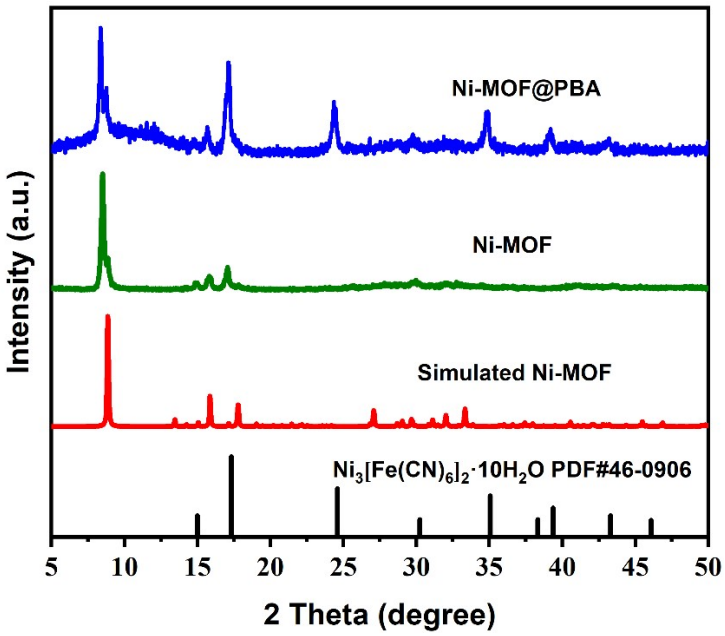

Fig. S4. XRD patterns of Ni-MOF and Ni-MOF@PBA.

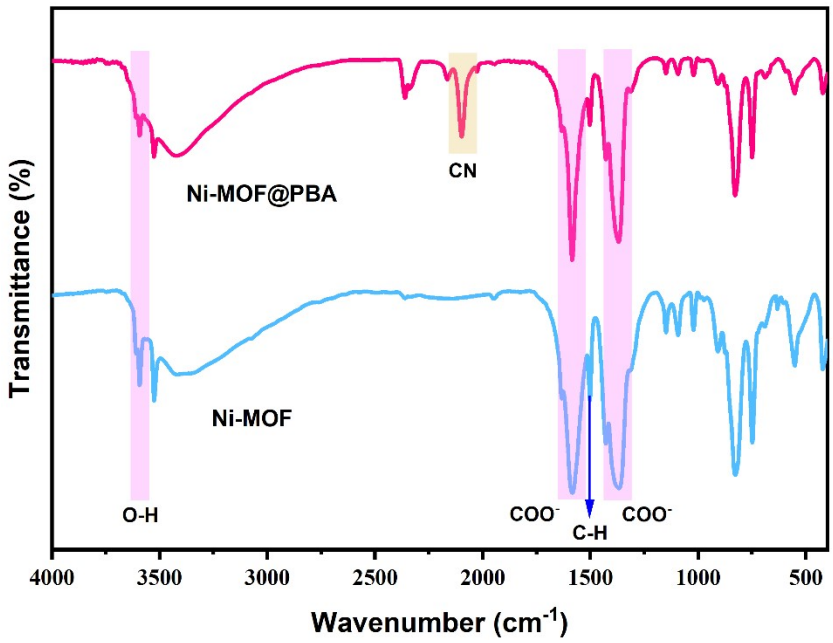

Fig. S5. FT-IR spectra of the as-obtained Ni-MOF and Ni-MOF@PBA.

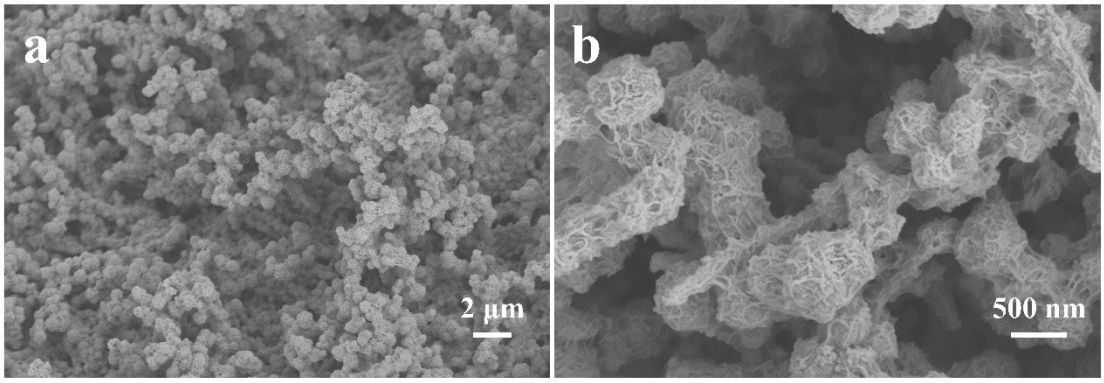

Fig. S6. SEM images of Ni_3S_2/NF.

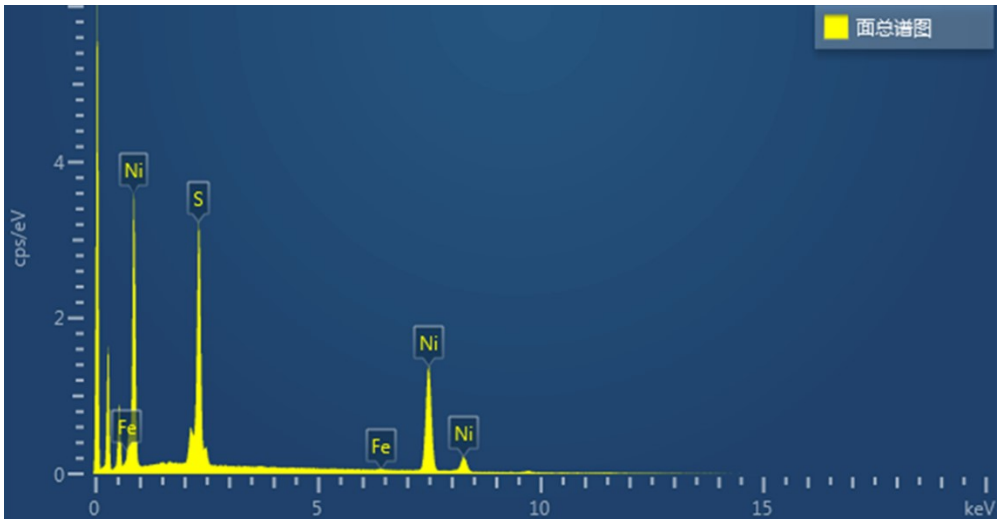

Fig. S7. EDS pattern of the soaked Fe-Ni_3S_2/NF.

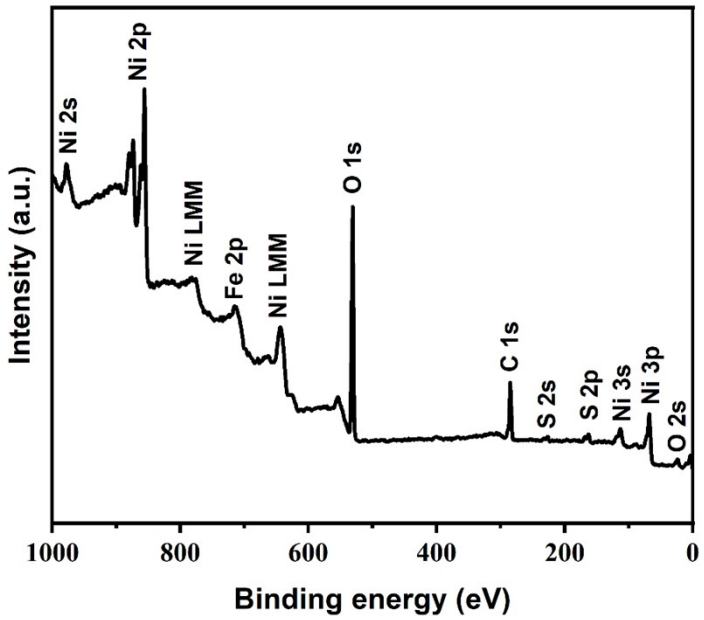

Fig. S8. XPS spectra of Fe-Ni_3S_2/NF survey scan.

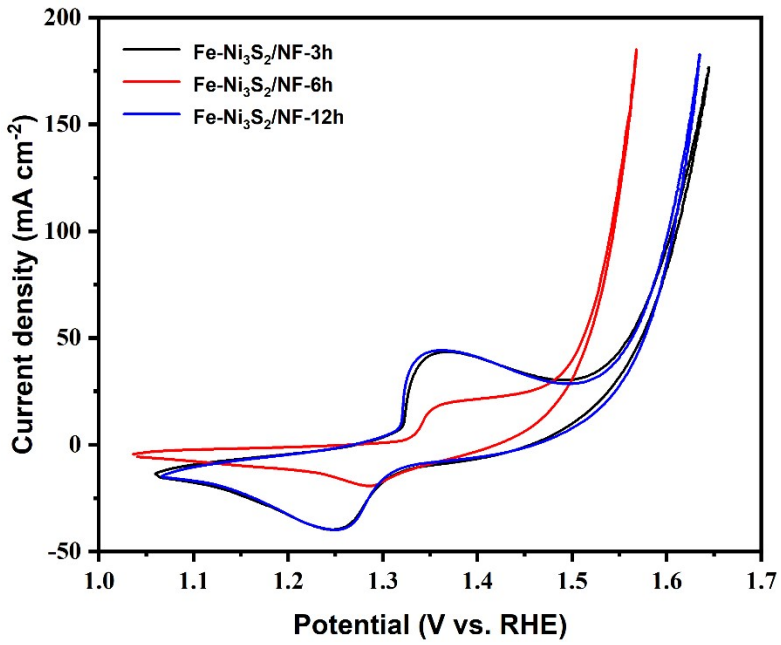

Fig. S9. Full CVs of Fe-Ni_3S_2/NF electrocatalysts at different in situ cation exchange reaction times for the OER in 1 M KOH at 5 mV s^{-1}**.**

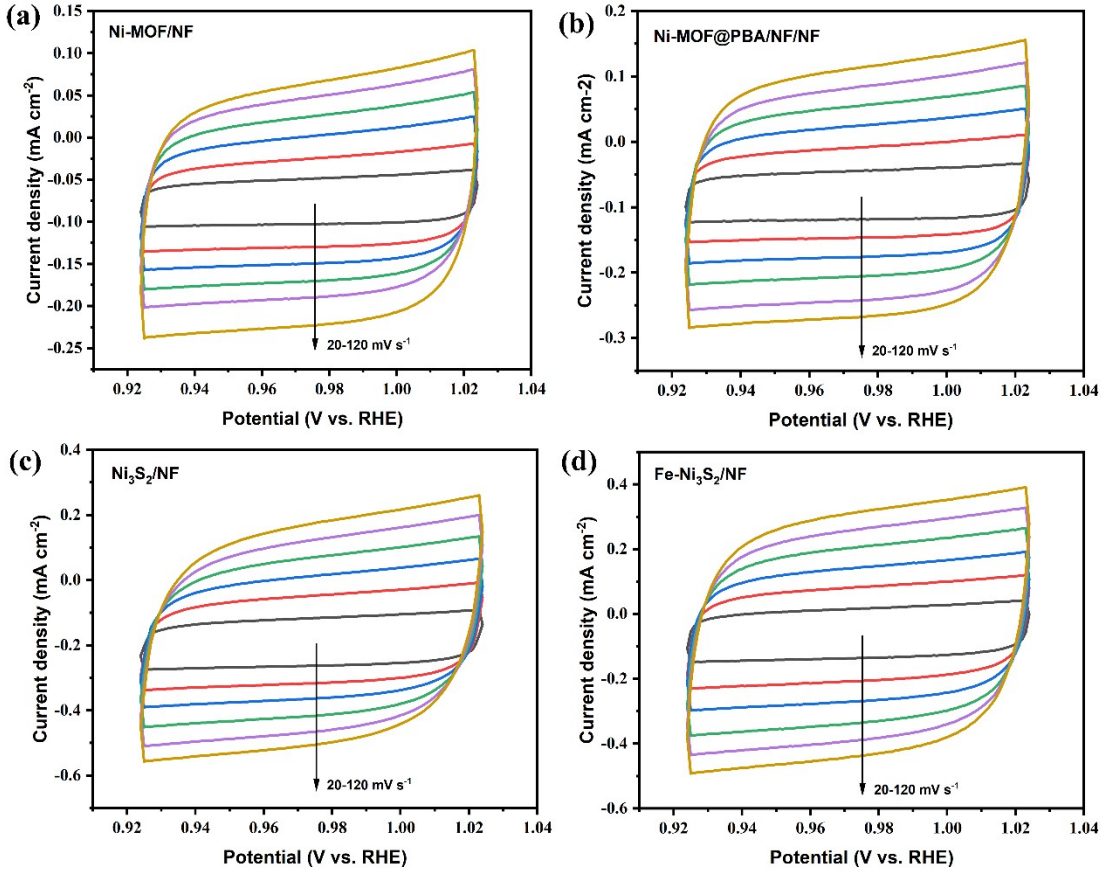

Fig. S10. CV curves of the NF, Ni-MOF@PBA/NF, Ni_3S_2/NF and the Fe-Ni_3S_2/NF at different scan rate of 20, 40, 60, 80, 100 and 120 mV·s^{-1}.

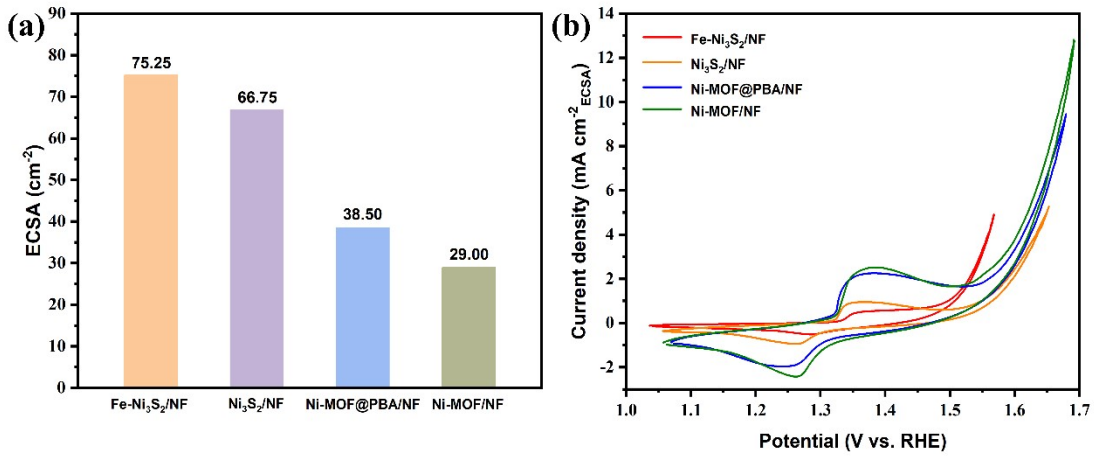

Fig. S11. (a) ECSA, and (b) ECSA-normalized OER activity of Fe-Ni_3S_2/NF, Ni_3S_2/NF, Ni-MOF@PBA/NF, Ni-MOF/NF.

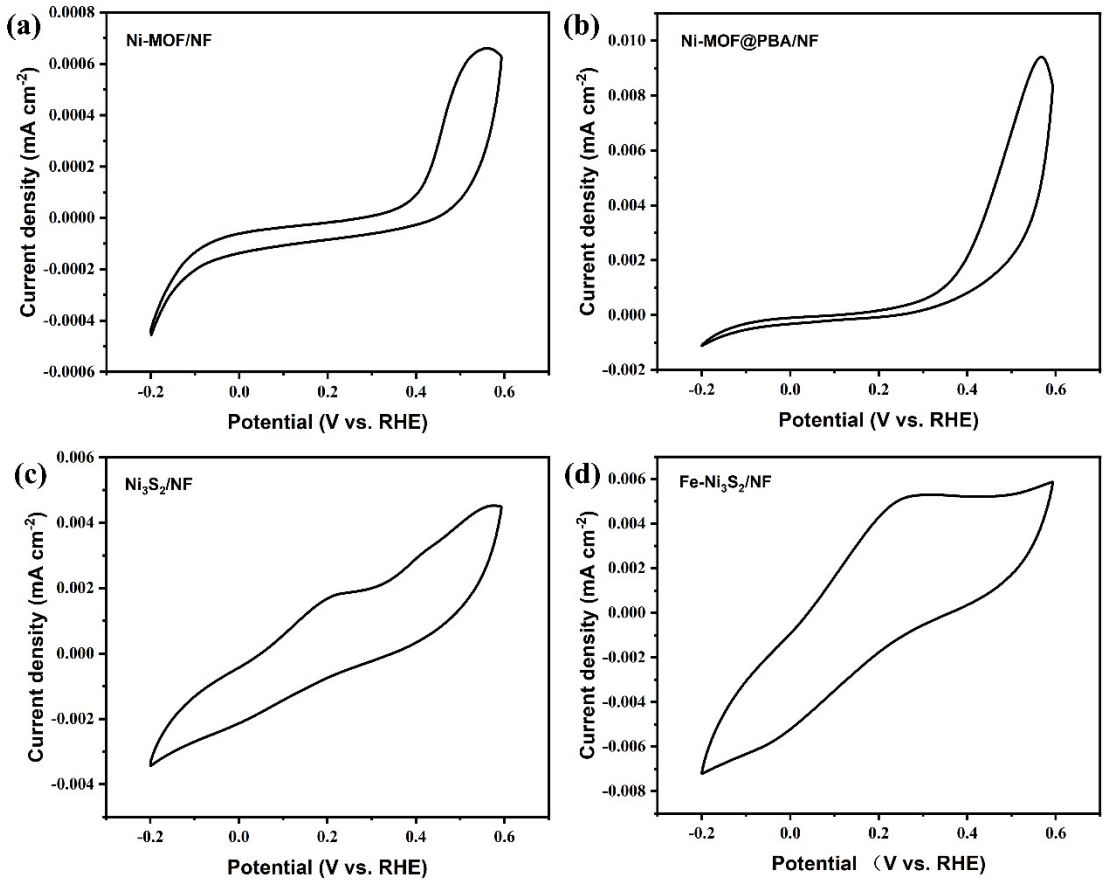

Fig. S12. CV curves of (a) Ni-MOF/NF, (b) Ni-MOF@PBA/NF, (c) Ni_3S_2/NF and (d) Fe-Ni_3S_2/NF in PB (pH = 7.0) at a scan rate of 50 mV s^{-1}.

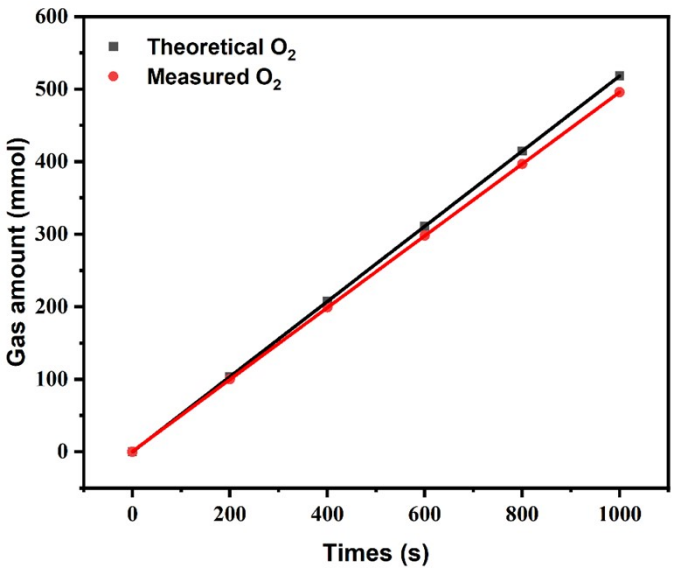

Fig. S13. The Faradaic efficiency of OER.

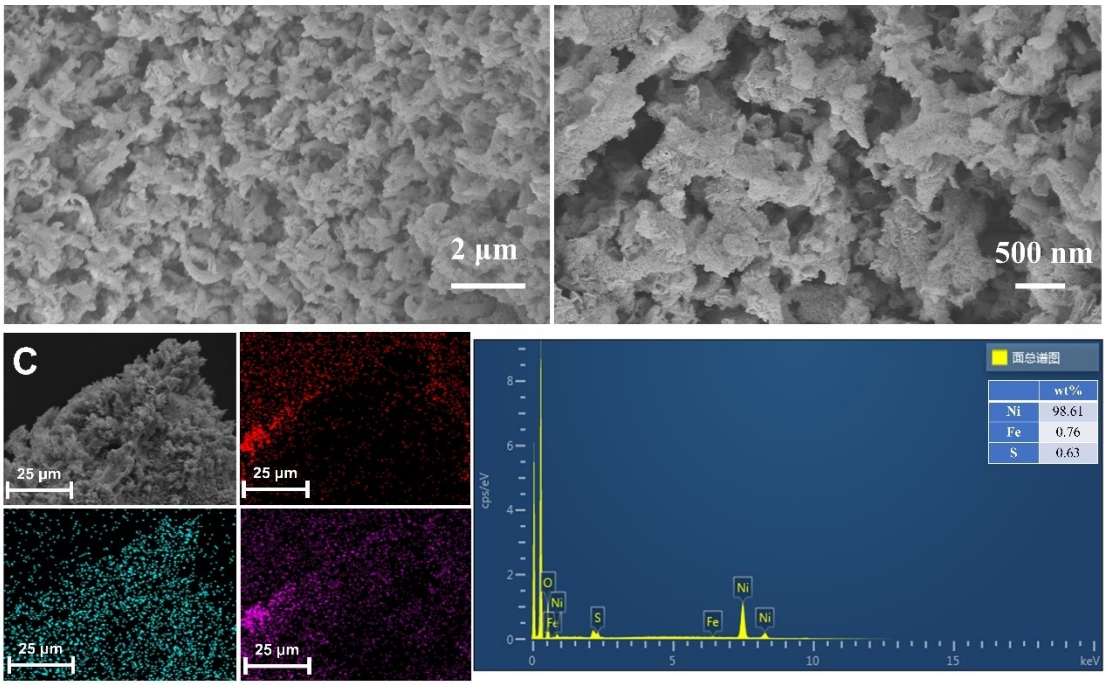

Fig. S14. (a, b) SEM images of Fe-Ni_3S_2/NF after OER. (c) The EDS elemental analysis of Fe-Ni_3S_2/NF after OER.

Table S1. Comparison of OER activity of Fe-Ni_3S_2/NF (red words) and recently reported Ni_3S_2 based electrocatalysts.

Catalysts	Support	Electrolyte	J/mA cm^{-2}	Overpotential/ mV	Tafel/ mV dec^{-1}	Ref.
Fe-Ni_3S_2	NF	1.0 M KOH	10	232	83.69	This work
G@Ni_3S_2	NF	1.0 M KOH	10	249	98.2	[S1]
Ni_3S_2@Ni	CC	1.0 M KOH	10	290.9	101.26	[S2]
F-Ni_3S_2	NF	1.0 M KOH	10	239	36	[S3]
Cu-Ni_3S_2	NF	1.0 M KOH	10	259	54.9	[S4]
Ni_3S_2-CeO_2	NF	1.0 M KOH	20	264	146	[S5]
NiFeCuP@Ni_3S_2	NF	1.0 M KOH	10	230	42	[S6]
Ni_3S_2@Ni_5P_4	NF	1.0 M KOH	50	399	75	[S7]
Ni_3S_2-Co_9S_8	NF	1.0 M KOH	20	294	80	[S8]
Bi_2S_3/Ni_3S_2	NF	1.0 M KOH	10	268	82	[S9]
Ni-Fe-OH/Ni_3S_2	NF	1.0 M KOH	10	268	54	[S10]
Cu_2S-Ni_3S_2	NF	1.0 M KOH	10	329	44.11	[S11]
Co-Ni_3S_2	NF	1.0 M KOH	20	297	50.3	[S12]
Fe–Ni_3S_2/rGO	NF	1.0 M KOH	20	247	63	[S13]
Ni_3S_2@$Co(OH)_2$	NF	1.0 M KOH	10	257	63.1	[S14]
NiFe LDH@Ni_3S_2	NF	1.0 M KOH	20	271	77	[S15]
NiO-Ni_3S_2	NF	1.0 M KOH	20	290	75	[S16]
Co_3O_4@Ni_3S_2	NF	1.0 M KOH	20	260	121.7	[S17]
Ni_3S_2/MnO_2	NF	1.0 M KOH	10	260	61	[S18]

NF: Nickel foam; CC: Carbon Cloth.

Table S2. Resistance values of various samples at 1.524 V *vs.* RHE.

Catalysis	R_s/Ω	R_{ct}/Ω
Ni-MOF /NF	1.32 Ω	3.46 Ω
Ni-MOF@PBA/NF	1.36 Ω	2.94 Ω
Ni_3S_2/NF	1.34 Ω	2.40 Ω
Fe-Ni_3S_2/NF	1.34 Ω	1.27 Ω
NF	1.36 Ω	101.00 Ω

References

S1. C. L. Jin, N. Zhou, Y. L. Wang, X. Li, M. Chen, Y. Z. Dong, Z. S. Yu, Y. N. Liang, D. Y. Qu, Y. L. Dong, Z. Z. Xie and C. C. Zhang, *J. Electroanal. Chem.*, 2020, **858**, 113795.

S2. H. Qian, B. X. Wu, Z. W. Nie, T. T. Liu, P. Liu, H. He, J. H. Wu, Z. Y. Chen and S. G. Chen, *Chem. Eng. J.*, 2021, **420**, 127646.

S3. Q. C. Xu, M. S. Chu, M. M. Liu, J. H. Zhang, H. Jiang and C. Z. Li, *Chem. Eng. J.*, 2021, **411**, 128488.

S4. H. Y. Liu, Z. X. Guo and J. S. Lian, *J. Solid State Chem.*, 2021, **293**, 121776.

S5. Q. Wu, Q. P. Gao, L. M. Sun, H. M. Guo, X. S. Tai, D. Li, L. Liu, C. Y. Ling and X. P. Sun, *Chin. J. Catal.*, 2021, **42**, 482-489.

S6. M. Khodabakhshi, S. M. Chen, T. Ye, H. Wu, L. Yang, W. F. Zhang and H. X. Chang, *ACS Appl. Mater. Interfaces*, 2020, **12**, 36268-36276.

S7. S. Khan, T. Ali, X. F. Wang, W. Iqbal, T. Bashir, W. Chao, H. Sun, H. L. Lu, C. L. Yan and R. M. Irfan, *Chem. Eng. Sci.*, 2022, **247**, 117020.

S8. R. Zhang, L. Z. Cheng, Z. Wang, F. Y. Kong, Y. Tsegazab, W. X. Lv and W. Wang, *Appl. Surf. Sci.*, 2020, **526**, 146753.

S9. S. Wang, W. D. Xue, Y. Fang, Y. Q. Li, L. L. Yan, W. J. Wang and R. Zhao, *J. Colloid Interface Sci.*, 2020, **573**, 150-157.

S10. W. J. He, G. Ren, Y. Li, D. B. Jia, S. Y. Li, J. N. Cheng, C. C. Liu, Q. Y. Hao, J. Zhang and H. Liu, *Catal. Sci. Technol.*, 2020, **10**, 1708-1713.

S11. K. S. Bhat and H. S. Nagaraja, *ChemistrySelect*, 2020, **5**, 2455-2464.

S12. X. Tong, Y. Li, N. Pang, Y. H. Qu, C. H. Yan, D. Y. Xiong, S. H. Xu, L. W. Wang and P. K. Chu, *Chem. Eng. J.*, 2021, **425**, 12.

S13. D. M. Shao, P. W. Li, R. Z. Zhang, C. H. Zhao, D. Q. Wang and C. J. Zhao, *Int. J. Hydrog. Energy*, 2019, **44**, 2664-2674.

S14. S. P. Wang, L. Xu and W. X. Lu, *Appl. Surf. Sci.*, 2018, **457**, 156-163.

S15. X. Q. Liang, Y. H. Li, H. Fan, S. J. Deng, X. Y. Zhao, M. H. Chen, G. X. Pan, Q. Q. Xiong and X. H. Xia, *Nanotechnology*, 2019, **30**, 9.

S16. L. S. Peng, J. J. Shen, X. Q. Zheng, R. Xiang, M. M. Deng, Z. X. Mao, Z. P. Feng, L. Zhang,

L. Li and Z. D. Wei, *J. Catal.*, 2019, **369**, 345-351.

S17. Y. Q. Gong, Z. F. Xu, H. L. Pan, Y. Lin, Z. Yang and X. Q. Du, *J. Mater. Chem. A*, 2018, **6**, 5098-5106.

S18. Y. Xiong, L. L. Xu, C. D. Jin and Q. F. Sun, *Appl. Catal. B-Environ.*, 2019, **254**, 329-338.